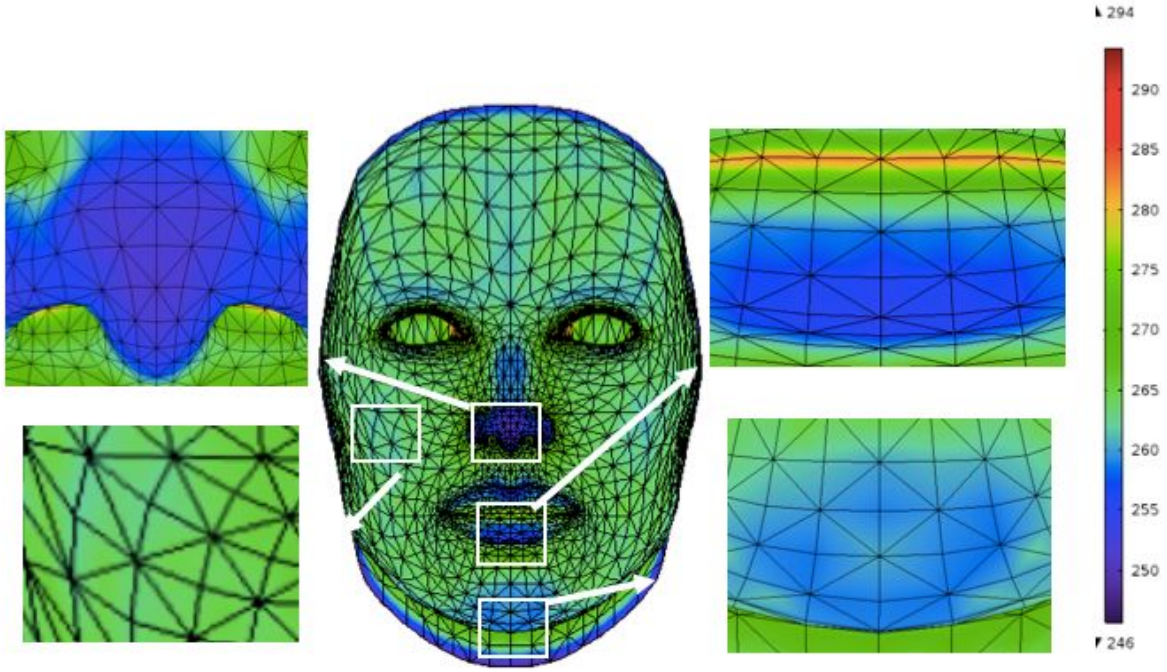

The Effect of Face Topography on Frostbite

BEE 4530

Fang Chen, Zhongling Huan, Sarah Kendl, and Alejandra Cambonchi

Dr. Datta

5/13/19

1. Executive Summary

Winters in most countries within the Northern hemisphere, which include heavily populated regions of Russia, Canada, China, and the United States, are commonly known to be harsh, unforgiving, and unpredictable. Cold weather injuries such as frostbite can occur within only a few minutes of exposure to extremely cold temperatures and high wind chill. We seek to provide a quantitative model of the effects of extremely cold and freezing temperature on the face and the extent of damage to tissue over time. In this study, our model will take into account the airflow of cold temperature on the face and the convective heat given off by the face. Using the duo model, we will be able to show the severity of tissue damaged.

In this study, we consider both the tissue temperature on the face and the temperature of the airflow. To investigate the mechanism of forced convection heat extraction in the face, we will use COMSOL, a multiphysics finite element analysis and simulation software, to develop a simple geometry of the face and replicate the heat exchanging properties when exposed to extreme temperature conditions. Our model will be a 3D simulation of the face with boundary conditions a close distance away from the face. We are primarily focused on simulating that the airflow is coming directly in front of the face and that is where the primary damage will occur. We will use the data provided by the National Weather Service that demonstrates how quickly hypothermia and frostbite can occur depending on the windchill and temperature.

The model will demonstrate the extent of damage that can occur in varied temperature settings. It will simulate how long the body can retain thermal energy while convective heat loss is simultaneously occurring. This model will allow us to demonstrate the importance of preventative care during extreme temperature conditions to avoid frostbite. It will allow us to quantitatively demonstrate how much tissue is damaged to help diagnose and treat frostbite cases.

2. Introduction

Winters in most countries within the Northern hemisphere, which include heavily populated regions of Russia, Canada, China, and the United States, are commonly known to be harsh, unforgiving, and unpredictable. Large temperature drops may occur in a matter of minutes, and in some cases, people have suffered severe frostbite when caught unaware by rapidly falling temperatures or rapid increases in windchill. Frostbite can occur within minutes depending on factors such as wind speed and ambient temperature. An average of 1,301 deaths per year occur in the United States alone due to frostbite coupled with exposure, with most of those deaths concentrated in Northern regions of the United States ("Quick Stats: Number of Hypothermia-Related Deaths," 2013). Polar vortexes, wide expanses of swirling cold air that originate from low pressure areas in the North pole, are becoming more common in these areas. Chicago, Illinois experienced a polar vortex in the winter of 2019 with wind chills as low as -50 degrees Fahrenheit. In temperatures that low, it can take as little as 5 minutes to develop the first stages of frostbite (Pierre-Louis, 2019).

Frostbite occurs when the moisture in organic tissue freezes and crystallizes causing the cells within the tissue to rupture, eventually causing apoptosis. The effect of frostbite increases with time of exposure. Frostbite most commonly occurs on the face, ears, feet, and hands and as exposure time increases, the symptoms of frostbite progress. In the first stage of frostbite, numbness, tingling, and pain can be felt in exposed areas of skin. As exposure time increases, the skin reddens and feels warmer than normal skin temperature as the body increases blood flow to the affected area in an attempt to increase its temperature. The second stage occurs after the initial freezing of tissue and it is in this stage that frostbite poses an even greater physiological risk as the heart rates begin to spike as the body attempts to stay as warm as possible. The third stage of frostbite occurs if prolonged freezing of tissue continues. All layers of the skin may be affected as the tissue continues to freeze. The exposed area turns white or bluish gray and all sensation of cold is lost. Joints or muscles may no longer work. After prolonged exposure, the skin may turn black and harden due to tissue death within the affected area ("Frostbite," n.d).

The danger of frostbite is well documented but precise information is unavailable on the duration of exposure that specific areas of the face could tolerate. This study focuses on the face, as frostbite injuries to the face are more common since people tend not to take as many precautions to protect their face from exposure, along with the fact that facial injuries caused by frostbite tend to be the most disfiguring. This study of frostbite seeks to provide a quantitative model of the effects of extremely cold and freezing temperature on the face and the extent of damage to tissue over time.

The phenomenon of cold wind blowing on an individual's face can be modeled utilizing the principles of laminar boundary layers, but facial topography does present some interesting challenges. Consider the wind as a uniform flow called a free stream velocity. The presence of an individual in the path of this flow affects the velocity and temperature of the fluid (air) particles. This causes the creation of velocity/momentum and temperature/thermal boundary layers, or regions of the flow that are affected by the presence of the individual. Due to face

topography, these layers will vary depending on the facial region (i.e. the cheeks, nose, etc.). As the distance traveled by the particles across the face increases, the boundary layers grow as they approach uniform temperature and free stream velocity. The thermal boundary layer's thickness governs heat transfer, thus altering the value of the heat transfer coefficient. Generally, as the thermal boundary layer thickness increases, the heat transfer coefficient decreases (Nellis & Klein, 2009).

The goal of this project is to illustrate how the thermal and velocity boundary layers vary depending on the facial region. There are no recent studies on record that have identified, through the use of 3D simulation tools, the particular sub-regions of the face that are most susceptible to frostbite. The face is particularly difficult to model and investigate due to its complex topography that includes numerous contours, changes in skin thickness, variations blood flow and the resultant variations in temperature. Through modeling and simulations, we can study frostbite at several different levels and layers of abstraction despite the number of variables, allowing a better understanding of the phenomena of frostbite and how to determine an accurate exposure threshold. The velocity obtained for several facial regions in the fluid flow simulation will be utilized to investigate heat transfer from the individual's face to the cold air. In addition, the heat transfer coefficient will also be investigated for each facial region. The model will identify the facial sub-regions most susceptible to frostbite through simulation and utilize the findings to develop strategies to reduce the yearly occurrences of frostbite.

2.1 Problem Statement

The purpose of this study is to investigate the facial regions most susceptible to frostbite upon prolonged exposure to cold winds. The tissue temperature will be analyzed as exposure time is increased for each defined facial region utilizing simulation tools. Currently, no recent studies have utilized simulation tools to identify the particular sub-regions of the face that are most susceptible to frostbite. The simulation procedure utilized in this study may provide a template for facial model implementation on modeling and simulation platforms such as COMSOL. These findings will be utilized to prevent frostbite by determining a maximum exposure threshold for each facial region.

2.2 Design Objectives

Due to the complexity of the vascular networks within the face and complex facial topography, a simplified model must be developed that preserves the physical response of tissue freezing through fluid flow and heat transfer. Both the functional and nonfunctional qualities, or design objectives, of our design must be considered in order to create a model that can accurately simulate the effects of frostbite. The following design qualities will be included in the development of our simulation and its associated mathematical model;

1. The phenomenon of facial tissue freezing shall be modeled utilizing a 3-D model of the face with realistic measures for skin thickness and metabolic heat.
2. The regions of the face most susceptible to frostbite shall be determined through the investigation of heat transfer dynamics.
3. The results of simulation shall be utilized to decrease occurrences of frostbite.

2.3 Design Assumptions

1. The front and the back surfaces were set to be the inlet and the outlet and the other surfaces surrounding the 3-D face mode shall be open.
2. Temperature flux outside the surface boundaries of the 3-D face model shall be zero.
3. The principles of laminar boundary layers shall be utilized as foundational principles.
4. The facial model shall undergo simulations of exposure to cold winds through the usage of COMSOL.
5. The facial regions shall be determined through the investigation of fluid flow dynamics.
6. The mathematical model for fluid flow integrated into the fluid flow simulation shall utilize a realistic value for the viscosity.
7. The mathematical model for heat transfer integrated into the heat transfer simulation shall utilize realistic values for heat capacity and conductivity.
8. The simulations shall be performed in a fixed volume.

3. Methods

Modeling of heat transfer and fluid flow was accomplished within COMSOL using the following geometry, governing equations, boundary conditions, and initial conditions. The model mimics the wind tunnel experiment to study the effects of wind speed and temperature on the facial formation of frostbite within a constricted space with an inlet and an outlet for air flow. Wind tunnels are large tubes with moving air inside generally utilized to study how air flows across an object. In our wind tunnel experimental set-up, a three-dimensional model of the face was imported into an open-ended box which served as the tunnel and the air flow across the face was investigated. The boundaries were set to open within COMSOL in order to avoid restriction of airflow around the face. This allowed the replication of the conditions in which frostbite may naturally occur in open space under high speed wind conditions at low temperatures, which are the conditions in which frostbite most commonly occurs.

3.1 Model Method and Schematics

In this specific study, a three-dimensional schematic was utilized. A 3-D model of the face was obtained from a 3-D model database. The thickness of the facial model used varied from 1.1 to 2.68 mm. The effects of varying thicknesses of the facial model were negligible on the formation of frostbite. This model was imported into COMSOL. It was placed in the center of an open-ended box, which served to replicate the tunnel structure in our wind tunnel experimental simulation. The dimensions of the open-ended box used were 1x1.1x1.3 ft, which were large enough to capture the changes in velocity as the incoming relative wind originating from the inlet makes contact with the face. The dimensions chosen were for the purpose of limiting the necessity of extensive processor power and computing time, while still making accurate calculations.

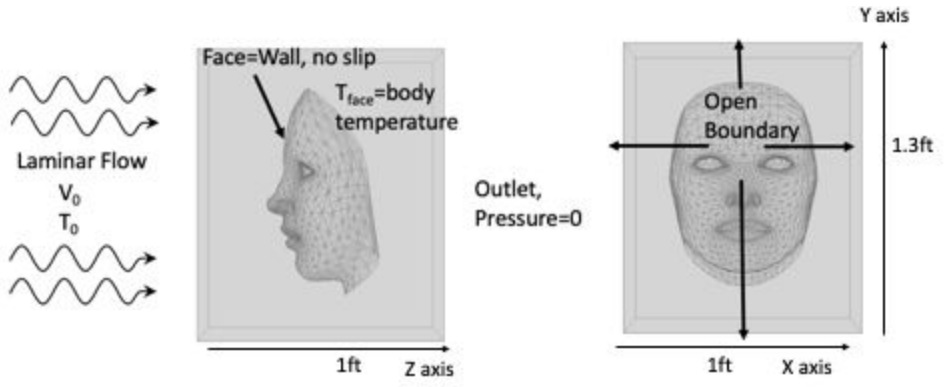

Figure 1. Schematic. Schematic of the human face and the surrounding air used to model the fluid flow and heat transfer. The schematic on the left is a side view and on the right is a front view of our schematic, includes the dimensions and the boundary conditions for the outer domain. Here, the inlet airflow is flowing in the z-direction and the outlet airflow is flowing out along the z-direction behind the face. For the boundary conditions of the outer domain, the surrounding planes in the Y-Z and X-Z directions are open boundaries.

3.2 Governing Equations

In order for frostbite to occur on the face in a simulated environment, the physics of fluid flow and heat transfer must be accounted for through the use of their respective governing equations. Frostbite formation depends upon the wind-speed, which corresponds to the fluid flow component of the simulation, and the temperature of the environment. Frostbite formation is also dependent on the decrease of the temperature of the skin as a result of exposure, which corresponds to the heat transfer component of our simulation.

The following fluid flow equation was used to model the air flow in all directions;

$$\rho(u * \nabla)u = \nabla * \left[-pI + \mu\left(\nabla u + (\nabla u)^T\right)\right] + F \tag{1}$$

where ρ is the density of the air, pI is the pressure force, μ is the viscosity of air, and F is the external force. The external force was maintained in the equation as a constant. The density term is shown below of Equation 1 was removed because it was assumed that air density did not vary.

$$\rho\nabla * (u) = 0 \tag{2}$$

The following heat transfer equation was used to model the heat loss in a three-dimensional space for the inner layers of the face;

$$\rho C_{pa}\frac{\partial T}{\partial t} = k\nabla^2 T + Q \tag{3}$$

where;

$$\nabla^2 T = \frac{\partial^2 T}{\partial x^2} + \frac{\partial^2 T}{\partial y^2} + \frac{\partial^2 T}{\partial z^2} \tag{4}$$

Equation 3 was utilized to model the heat loss of the face upon contact within the free stream velocity where ρ is the density of the face, C_{pa} is the apparent heat capacity of the face as its interstitial fluid transitions from unfrozen to frozen, k is the thermal conductivity of the face, and Q is the heat generation within the face due to blood flow. The following equation was used for the heat generation term in Equation 3.

$$Q = \rho_b C_b \dot{V}_b (T_a - T) + Q_{metabolic} \tag{5}$$

where ρ is the density of the blood, C_b is the heat capacity of the blood, $\dot{V}_b$ is the flow rate of the blood in m^3 of blood / m^3 of tissue per second, and T_a is the arterial temperature. The last term $Q_{metabolic}$ denotes the heat generated by the body's metabolism and ranges from 4 - 30 W/m^3.

For the surrounding domain around the face, the following equation was used for heat transfer;

$$\frac{\partial T}{\partial t} = \frac{k}{\rho C_p} \nabla^2 T \tag{6}$$

where, ρ is the density of the air, C_p is the heat capacity of the air, k is the thermal conductivity of the air.

3.3 Boundary and Initial Conditions

In order to mimic the conditions in which frostbite may naturally occur, realistic boundaries and initial conditions were utilized in the simulation. The planes surrounding the face in the Y-Z and X-Z directions were open boundaries to avoid restriction of air-flow. The simulation ran in a fixed volume in order to capture the changes in velocity as the free stream velocity made contact with the face. The air was only allowed to enter through the side of the box directly in front of the face and was only allowed to exit through the side behind the face. The full boundary conditions utilized in the COMSOL simulation are shown in Table 1.

Table 1. Boundary Conditions

Domain	Boundary	Condition	Basis
		Fluid Flow	
Air(1)	In Front of Face	Inlet $v = v_0$	A constant air flow onto the front of the face. There were three velocity values used for simulation: 4.47, 6.7, 13.41; unit is m/s
Air(1)	Back of Face	Outlet $P = 0\ Pa$	No pressure change i.e. no obstruction as air flow exits
Air(1)	Top, Bottom, Sides of Face	Open boundaries	Open boundary with no obstruction of air flow at sides of face
Face(2)	Entire face surface	No slip-penetration	Face was treated as a wall
		Heat Transfer	
Air(1)	In Front of Face	Temperature Boundary	Continuity of temperature and flux
Air(1)	Back of Face	Open Boundary	Continuous outflow of air
Air(1)	Top, Bottom, Sides of Face	Open boundaries	Open boundaries as in space

Note: the face domain 2 represents the entire three- dimensional face model

In addition, the dynamics of fluid flow and heat transfer for multiple free stream velocities originating from the inlet at different initial temperatures were analyzed. The temperature of the face was set to be 310.15 K, which is the average body temperature. The full initial conditions used in the formulation are given in Table 2.

Table 2. Initial Conditions

	Heat Transfer	
Domain 1, Inlet (Boundary at Front of Face)	Ambient temperature	From fluid flow simulation, three ambient temperature values were used for heat transfer. Temperature values used were 233.15, 238.71, and 241.48; unit is Kelvin
Domain 2 Face	$T_o = 310.15K$	At time equals 0, the temperature of the facial region is equal to the average body temperature (the cold wind was not begun to cool the face)

All of the boundary conditions, initial conditions, and input parameters shown in Tables 1 and 2 were inputted into COMSOL to perform the fluid flow and heat transfer simulations.

4. Results

4.1 Simulation Results

Airflow simulation:
Before the implementation of the heat transfer simulation, the airflow simulation within COMSOL was performed with three sets of initial free stream velocity. A wind tunnel experimental set-up was utilized to analyze the airflow around the face upon its contact with the free stream velocity. The air around the face was stationary before the free stream velocity began flowing from the inlet within the simulation. Figure 2 shows the velocity profiles of the front, side, and top views of the face.

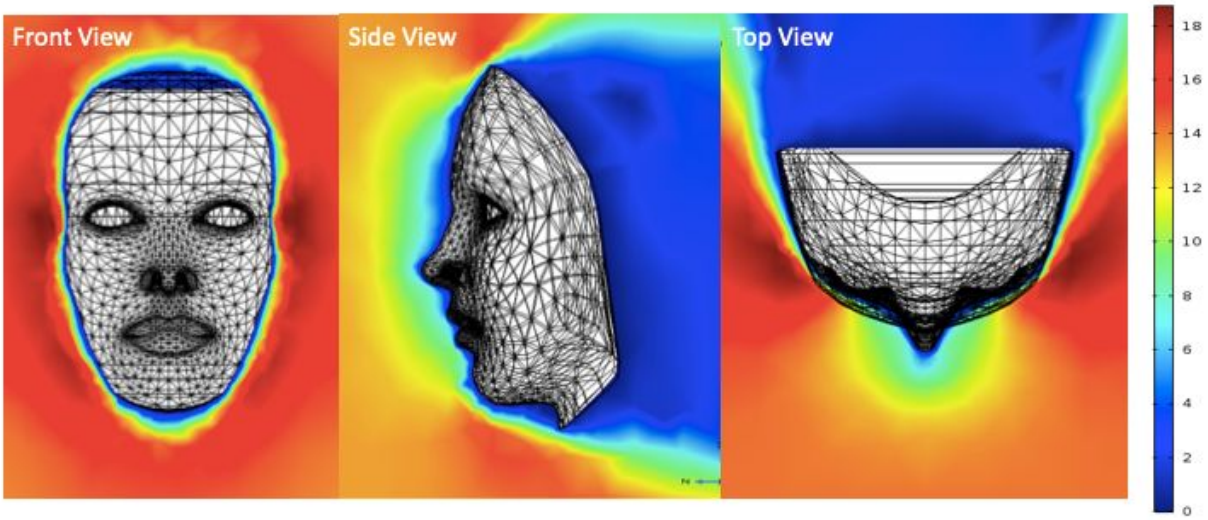

Figure 2. Results of the Air Flow Simulation. Velocity profiles of the front, side, and the face. This figure illustrates the stationary study of fluid flow for air flow with velocity of 13.41 m/s

All the views of the facial model obtained from the air flow simulation show a decrease in velocity in the region directly surrounding the face. This is illustrated by the dark blue color at the edge of the face, which indicates a velocity of 0 mph. This decrease of velocity occurred because the face acted as a wall or flat plate in the simulation, completely ceasing the flow of the free stream velocity. As the flow of air travels across the face after initial contact, the momentum boundary layers on the face increase until they return to initial free stream velocity magnitude. This is shown most clearly in the side view of the face in Figure 2. The dark blue region around the edge of the face shows an increase in velocity as illustrated by the surrounding light blue, yellow, and orange regions as the free stream velocity travels across the face. The orange color indicates that the free stream velocity has returned to its initial magnitude. These findings are consistent with the principles of laminar boundary layers. Figure 2 also indicates the occurrence of the Venturi effect in the simulation. This is illustrated most clearly by the dark red region next to the left and right cheeks in the front view of the face in Figure 2. The Venturi effect is the reduction of fluid pressure as a result of constricted air flow. Although open boundaries were utilized in COMSOL, the box surrounding the face used in the wind tunnel experimental set-up

still caused air flow constriction. These effects were deemed negligible because only frostbite formation on the surface of the face was of interest.

Heat transfer:
After the completion of the fluid flow simulation, the heat transfer simulation was performed within COMSOL. The simulation was run with the heat transfer in solids COMSOL setting. The temperatures of each facial region after a 300 second and 600 second exposure time was evaluated for varying combinations of initial magnitudes and temperatures of the free stream velocity originating from the inlet. Facial regions were naturally defined by the results of a heat transfer simulation with values of 233.15K at 4.47m/s, 241.48K at 6.7m/s, and 238.71K at 13.4m/s. Figure 3 shows the results of this heat transfer simulation with a wind speed of 13.41m/s and wind temperature of 238.706K. Areas of similar topography, such as the nose and lips, showed a similar decrease in temperature. The coldest facial regions of Figures 3 are labeled with white squares. The frostbite threshold was defined as a temperature below 25F (-4 degC).

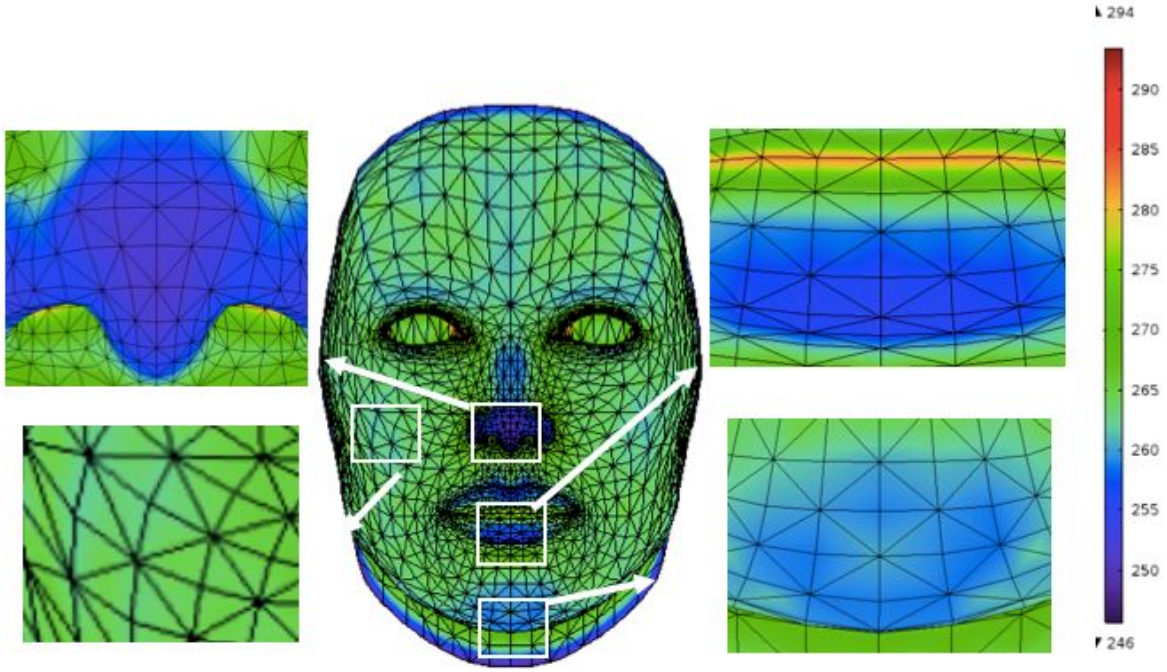

Figure 3 The temperature profile of face after 300 seconds exposure to a wind speed of 13.41m/s and wind temperature of 238.706K. The white squares indicate the facial regions that have the lowest temperature readings, which indicate these areas are the most susceptible to frostbite. On the top left corner, the nose has the lowest temperature compared to the other facial regions.

Figure 3 indicates that the nose, cheeks, lips, and chin are the regions most susceptible to frostbite. Thus, to better understand how temperature decreased with exposure time, the nose,

cheeks, and lips were analyzed. The temperature profiles were plotted for the following free stream velocities with an exposure time of 300s and 600s; 233.15K at 4.47m/s, 241.48K at 6.7m/s, and 238.71K at 13.4m/s. These temperature profiles are shown in Figures 4, 5, and 6. Note that only the temperature profile of the right cheek is shown due to its similarity in topography in the left cheek.

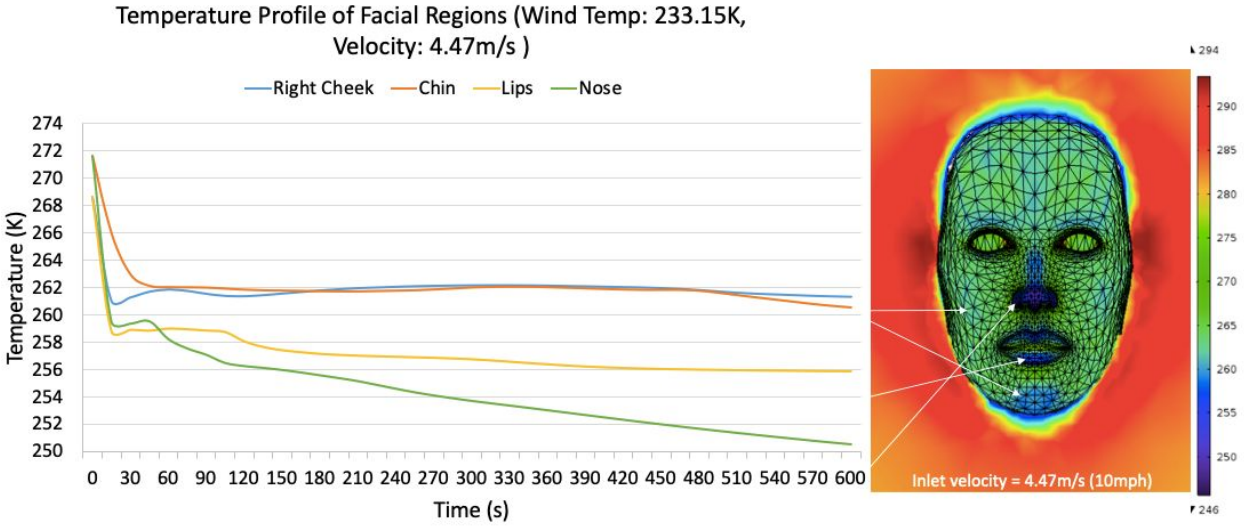

Figure 4 Temperature vs. time for Facial Regions when exposed to wind temperature of 233.15K and wind speed of 4.47m/s (-40F and 10mph). After 600s of exposure, temperature around the nose has the largest temperature drop and second largest drop is lips. Meanwhile the chin and right cheek have similar temperature drops.

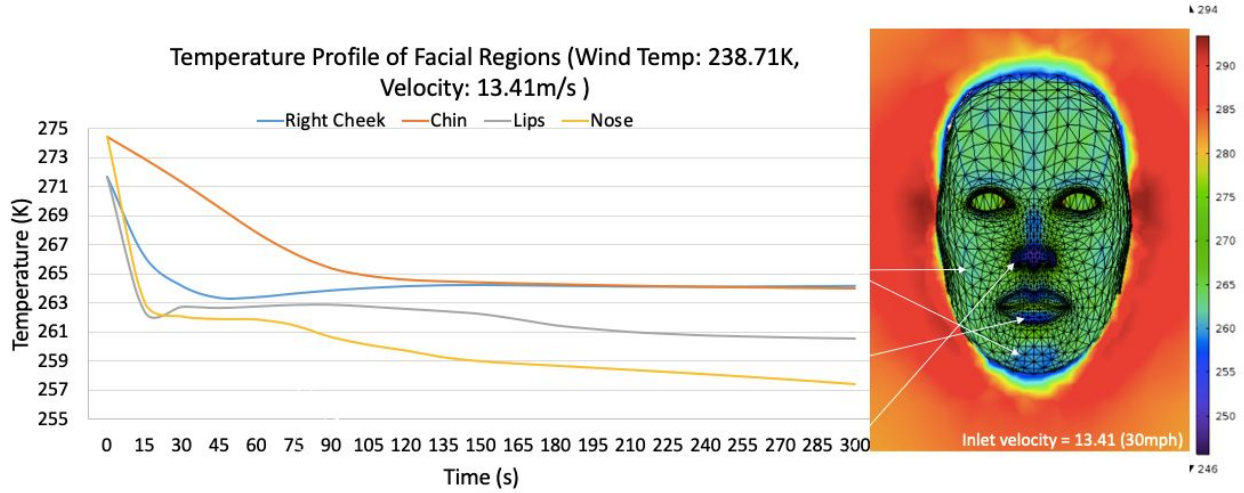

Figure 5 Temperature vs. time for Facial Regions when exposed to wind temperature of 238.7K and velocity of 13.41m/s (-30F and 30mph). After 300s of exposure, temperature around the nose has the largest temperature drop and second largest drop is lips. Meanwhile, again the chin and right cheek have similar temperature drops.

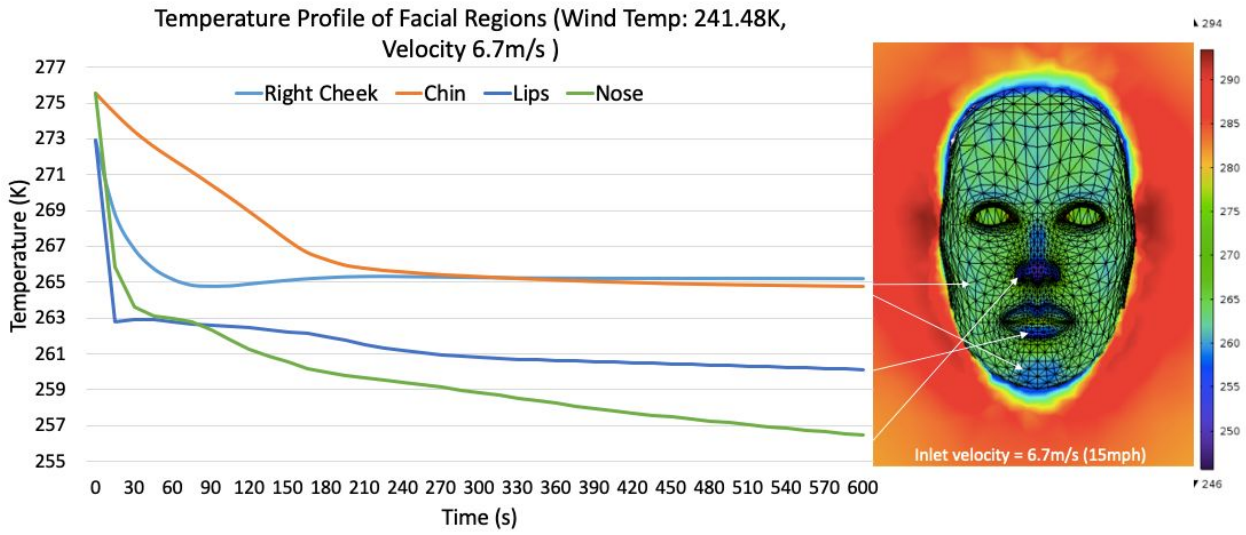

Figure 6 Temperature vs. time for Facial Regions when exposed to wind temperature of 241.48K and velocity of 6.7m/s (-25F and 15mph). After 600s of exposure, temperature around the nose has the largest temperature drop and second largest drop is lips. Meanwhile, again the chin and right cheek have similar temperature drops.

According to Mayo Clinic documentation, frostbite mostly occurs at nose, cheeks, and chin ("Frostbite," n.d.). This is consistent with experimental findings. According to Figures 4, 5, and 6, the nose showed the greatest susceptibility to frostbite as illustrated by the greatest temperature decrease over a given time. This may be due to the topography of the nasal region. Its prominent position causes it to experience the brunt of the stream velocity. Regions immediately around the nose may experience the free stream velocity after it has been slightly rewarmed by the body temperature. This rewarming causes an increase in the thickness of the temperature boundary layer. The cheeks were deemed the second most susceptible, followed by the chin and lips. The only region that indicated a larger susceptibility to frostbite according to Figures 4, 5, and 6 that cannot be validated is the lips. Due to the increased blood flow and heat generation of the lips, frostbite does not commonly occur in this region. In order to account for this factor in the heat transfer simulation and to better reflect biological phenomena, a larger heat generation term for the governing equation of the heat transfer within areas of the face with higher blood flow could be considered for future simulations.

4.2 Sensitivity Analysis

Sensitivity analysis is a technique that allows the determination of how changes in the independent variables affect the dependent variable. This allows the determination of the robustness of the model in the presence of uncertainty. For the sensitivity analysis, the responsiveness of the model to changes in heat capacity and conductivity was determined. The temperature of a node selected on the nose at t = 300s was evaluated as the material parameters

were increased and decreased. The values of apparent heat capacity (C_{pa}) and thermal conductivity (k) of the face were varied within the following ranges;

$$C_{pa}: \ 0.9C_{pa} - 1.1C_{pa}$$
$$k: \ 0.9k - 1.1k$$

Figure 9 illustrates the percent change in temperature of the nose at time=300s with varying apparent heat capacity and thermal conductivity. The initial temperature on the nose was set as 310.13 K. Table 3 shows the calculated percentage change in final temperature as the result of a ten percent increase and decrease of each parameter.

Table 3. Sensitivity Analysis of C_{pa} and k

Parameter	Temperature (K)	Percentage Change
1.1 C_{pa}	257.68	0.112%
1.0 C_{pa}	257.39	-
0.9 C_{pa}	256.98	-0.159%
1.1 k	257.02	-0.144%
1.0 k	257.39	-
0.9 k	257.76	0.144%

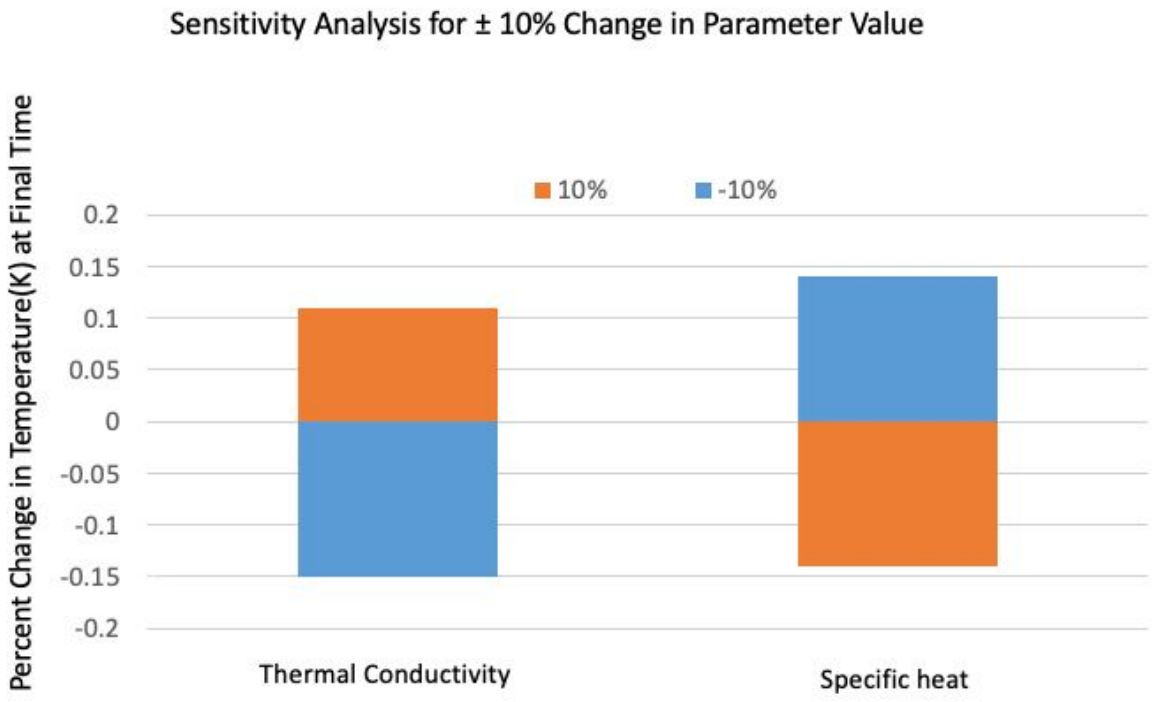

Figure 9. Plot of the sensitivity analysis.

As indicated by Table 3 and Figure 9, our model is robust to changes in the selected parameters. The percent change in final temperature for a 10% increase and decrease in heat capacity and conductivity is below 0.2%. As thermal conductivity was increased by 10%, the final temperature of the node on the nose decreased. In contrast, when thermal conductivity was decreased by 10%, the final temperature of the node increased. Thermal conductivity indicates the rate of conduction or the rate at which heat passes through a material. The higher the heat conductivity, the faster heat is lost. Thus, the higher the thermal conductivity, the lower the final temperature of the node. When heat capacity, or specific heat, was decreased by 10%, the final temperature of the node decreased. In contrast, as the heat capacity was increased by 10%, the final temperature of the node increased. Heat capacity is the number of heat units needed to raise the temperature of the material by one degree. If more heat is required to raise the temperature of a material, the material will show a lower temperature than one with a lower heat capacity under heating or warming conditions. Thus, the higher the heat capacity, the lower the temperature of the node.

5. Validation

To validate that the model provided results that accurately represented the biological phenomena of frostbite, data was collected from various sources to support experimental findings. In addition, the volume of frozen tissue at increasingly cold temperatures was also analyzed to ensure freezing of internal tissue increased with decreasing temperature, which is what would naturally occur in the human body.

In order to select the temperature and magnitudes of the free stream velocity for the heat transfer and fluid flow simulations, data collected from the National Weather Service dated 11/01/2001 was utilized (“Wind Chill Chart,” 2001). The National Weather Service, a research group, created a model to calculate the approximate time it would take for the human face to get frostbitten depending on the wind speed and the surrounding temperature. The model used a consistent standard for skin tissue resistance and assumed that there is no impact from the sun. These results are organized into a standardized chart seen in Figure 10.

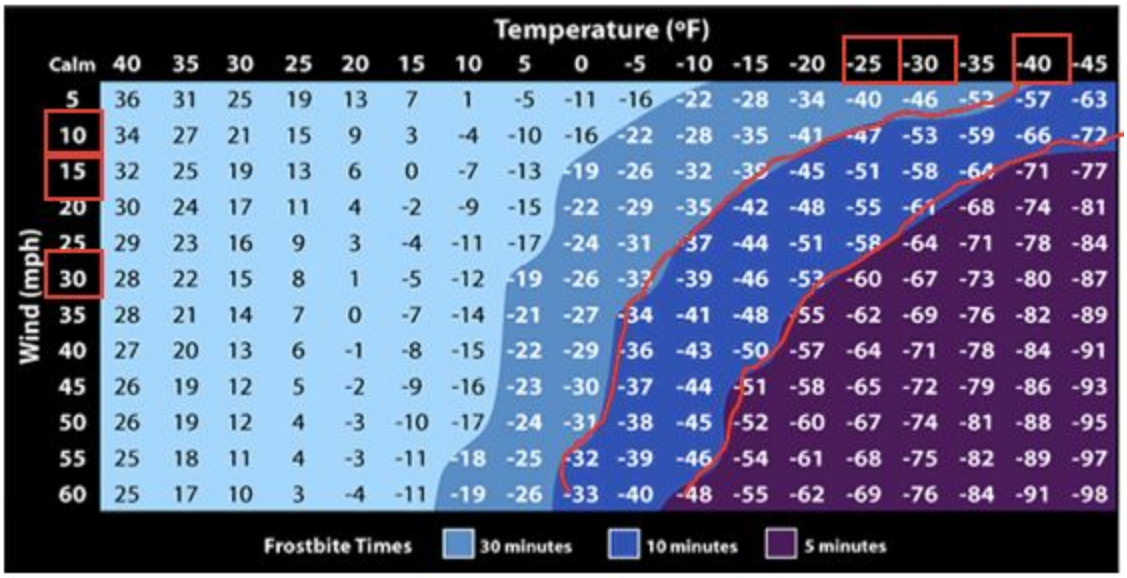

Figure 10.Wind Chill Chart. The National Weather Service data table for approximate time frostbite begins to forms depending on the combination of wind temperature and wind speed.

Our findings were consistent with the data generated by the National Weather Service. As shown in Figures 4, 5, and 6, temperatures of facial regions suggest the frostbite formation after exposure to preset wind velocities and temperatures that corresponds to the table above. For the simulation, we used 3 combinations from the table above: -40F at 10 mph, -25F at 15 mph, and -30F at 30 mph (233.15K at 4.47m/s, 241.48K at 6.7m/s, and 238.71K at 13.4m/s). For each combination, we ran the simulation for the duration of exposure mentioned above in the table. According to our temperature profiles of multiple facial regions, data collected showed similar trends of temperature change upon exposure as indicated by the Wind Chill Chart ("Wind Chill Chart," 2011). This indicates that the combination of wind temperature and speed does impact when frostbite starts to occur and how severe it gets. In addition, the findings were consistent with Mayo Clinic documentation which indicates that frostbite is most common on the nose, cheeks, and chin ("Frostbite," n.d.). Based on simulated results, the nose, cheek, and lips regions are among the regions most susceptible to frostbite, which matches expectations.

Additionally, we confirmed that the facial model utilized in our simulations appropriately generated bioheat due to blood flow as provided by the heat generation term in the heat transfer equation for the inner layers of the face. A node on the nose, the facial region most susceptible to frostbite, with increasing proximity to the nose and increasing penetration depth into the skin was chosen for analysis. Natural biological phenomena dictate that as proximity to the skin increases, temperature should also increase. In addition, as skin penetration depth increases, temperature should also increase. Temperature v distance was analyzed for initial temperatures of -10 to -40F. Distance is defined as arc length within COMSOL. Figures 11, 12, 13, and 14 graph temperature in K v arc length in ft for initial temperatures of -10, -20, -30, and -40F. Free stream velocity is 30 mph and exposure time is 300 s for all four figures. 0.012 ft is defined as the surface point on each graph, or the point on the surface of the nose. All larger arc lengths

(0.012- 0.05 ft) are under the surface of the skin. Temperatures evaluated for these arc lengths are of the external and internal tissue of the nose. All arc lengths below 0.012 ft (0-0.012 ft) are above the surface of the skin. Temperatures evaluated for these arc lengths are of the air directly above the node on the nose.

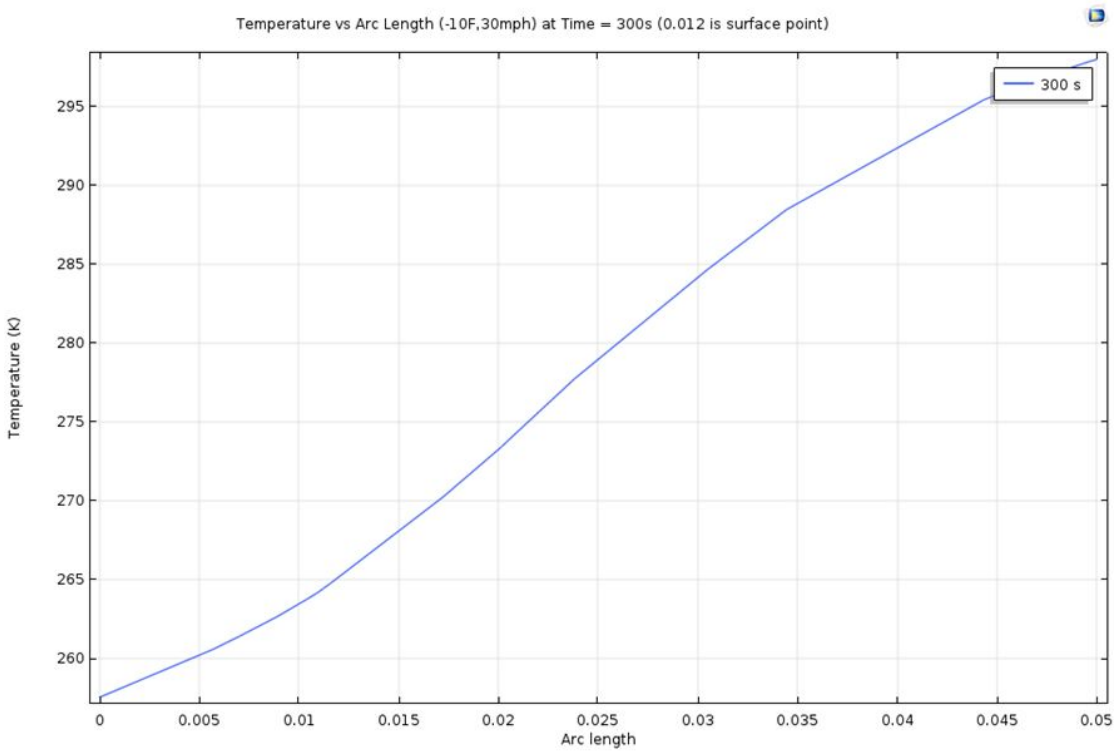

Figure 11. Temperature (K) v Arc length (ft). The graph was obtained using an initial temperature of -10F and an initial velocity of 30 mph.

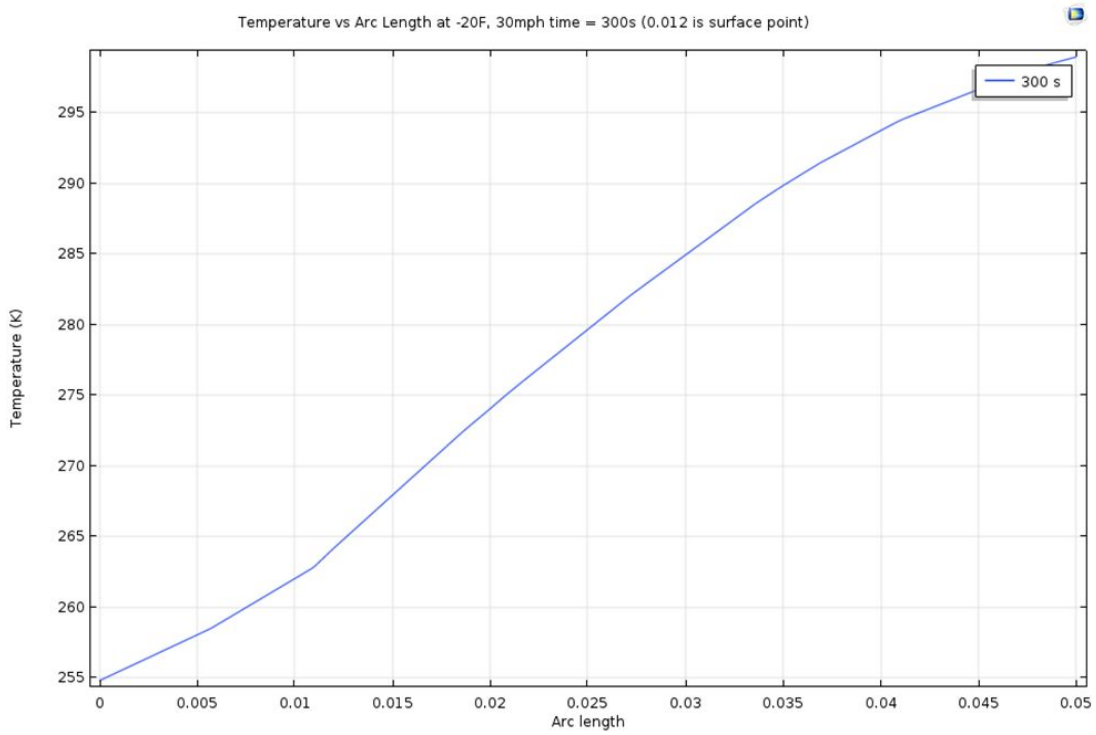

Figure 12. Temperature (K) v Arc length (ft). The graph was obtained using an initial temperature of -20F and an initial velocity of 30 mph.

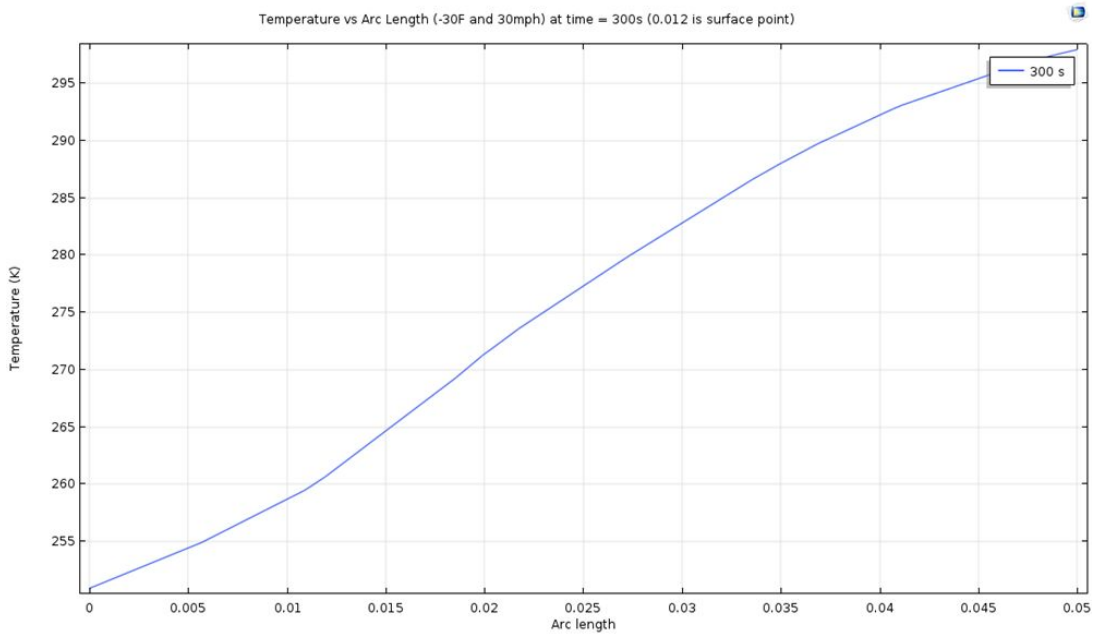

Figure 13. Temperature (K) v Arc length (ft). The graph was obtained using an initial temperature of -30F and an initial velocity of 30 mph.

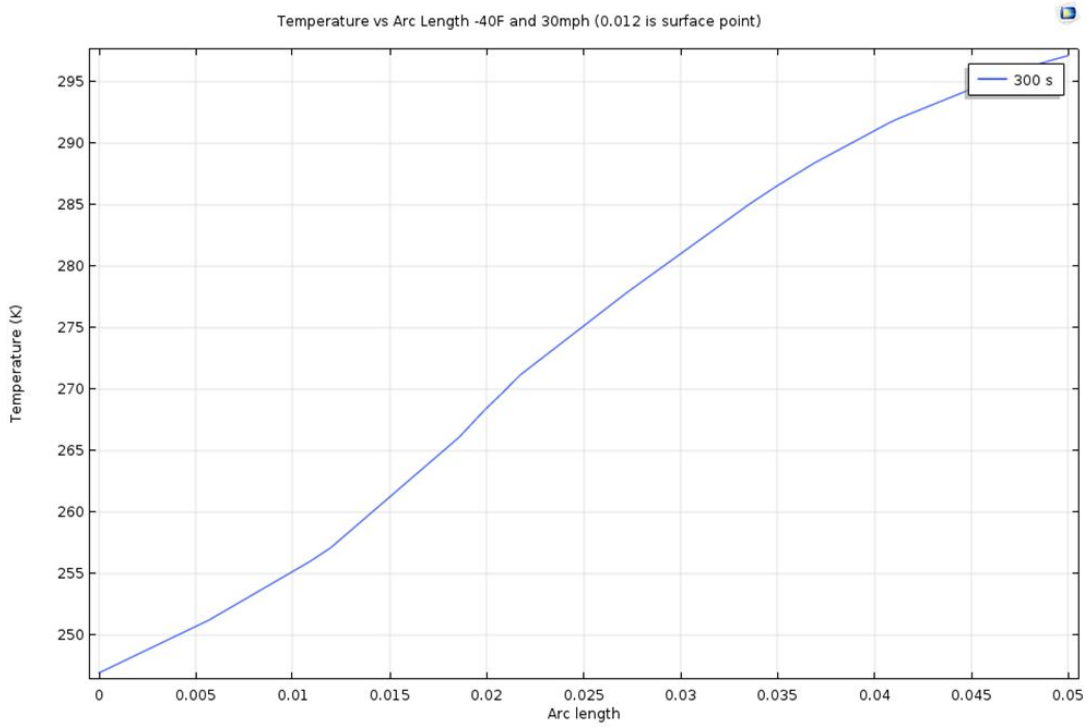

Figure 14. Temperature (K) v Arc length (ft). The graph was obtained using an initial temperature of -40F and an initial velocity of 30 mph.

All four figures shown above indicate that as arc length increases, temperature also increases. This is consistent with biological phenomena. This is because the air directly above the skin is warmed by bioheat generated by blood flow. As arc length continues to increase and penetrate the skin, the temperature further increases due to an increase in bioheat. Figures 11-14 also illustrate that the depth of tissue frozen increases with increasing temperature. Frozen tissue is defined as temperatures below 269 K. For example, 0.012-0.016 ft of tissue is frozen at -10F. In contrast, 0.012- 0.02 ft of tissue is frozen at -40F.

Volume of internal and external frozen tissue v temperature was also analyzed. Freezing of biological tissue is governed by the following equation;

$$Cpa = w[(1-f)Cpu + fCpi + \lambda_f \partial f/\partial T] + (1-w)Cps \quad (7)$$

where *Cpa* is total heat capacity, *w* is the initial water content as a fraction of total weight, *f* is the fraction of total water frozen, *Cpi* is the heat capacity of ice, *Cps* is the heat capacity of the solute, λ_f is the latent heat of freezing, and *Cpu* is the heat capacity of water. Figures 11-14 were utilized to find the volume of tissue frozen by assessing the volume of tissue analyzed by COMSOL for temperature v arc length plots. The volume was found by finding the approximate area of a node (.0008 ft x .0008 ft) and multiplying by the total arc length beneath the surface of the skin (0.012- 0.05 ft). The volume of tissue frozen was found by multiplying the approximate area of a node by the depth of tissue frozen, which was defined as a tissue temperature below

269 K. Figure 15 shows an illustration of this concept. Note that the curvature of the nose was ignored for simplicity.

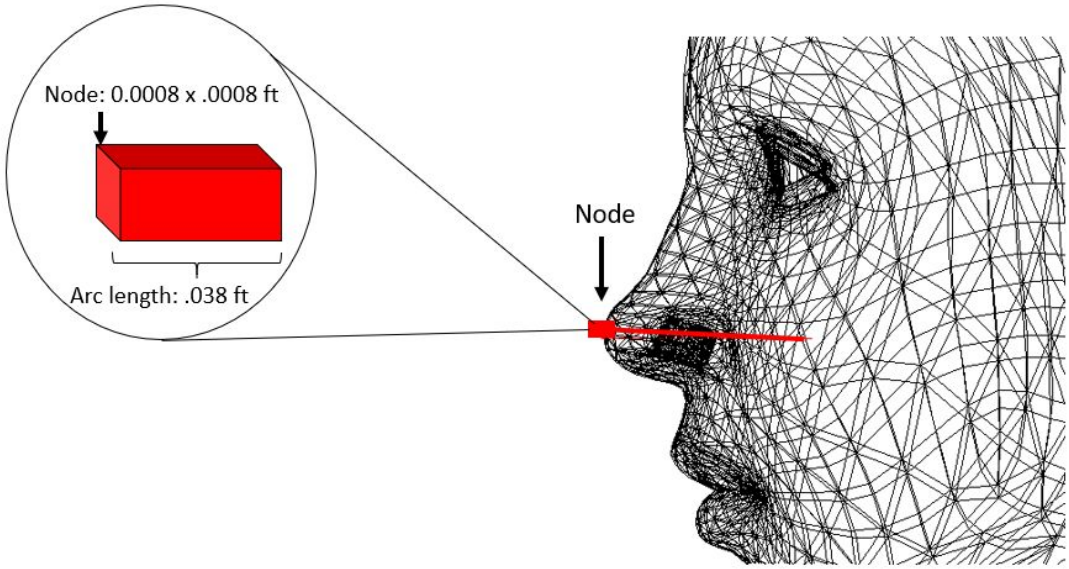

Figure 15. Volume based on Arc length. Tissue frozen was found within the volume shown above.

Figure 16 shows the approximate fraction of tissue frozen v decreasing temperature. The fraction of tissue frozen was found by dividing the volume of tissue below 269 K by the total volume of tissue within the defined region.

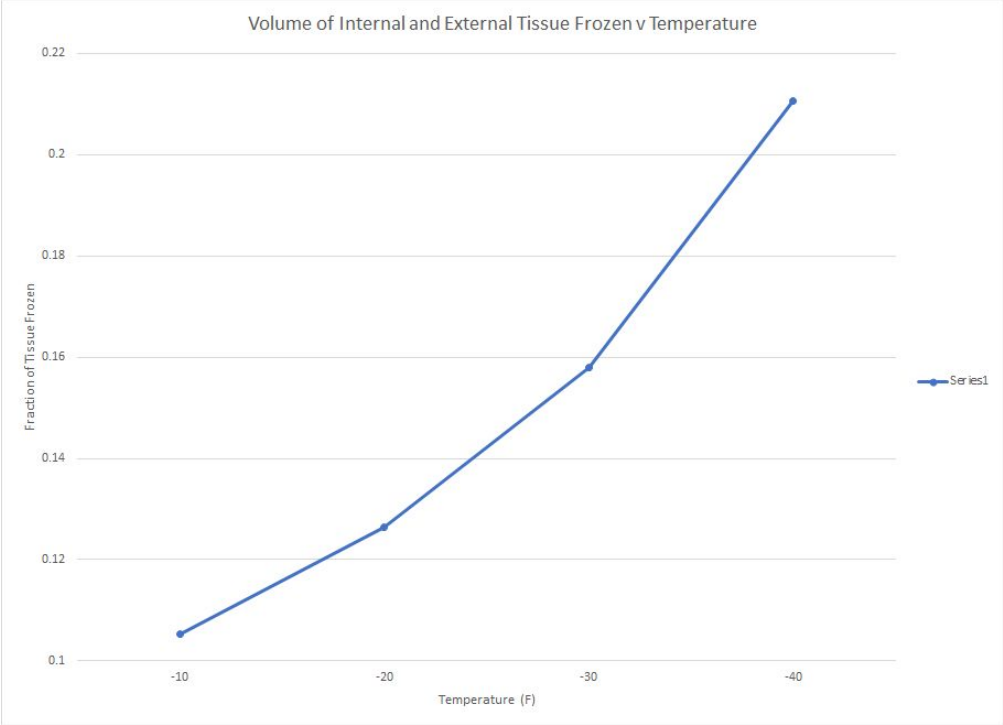

Figure 16. Volume of Internal and External Tissue Frozen v Temperature.

Figure 16 predictively shows that the fraction of tissue frozen increases with decreasing temperature, which is consistent with the increased formation of frostbite in human tissue in increasingly cold temperatures.

6. Conclusion

The data we collected from our fluid flow and heat transfer simulations may be utilized to determine the efficacy and environmental constraints of products marketed for frostbite prevention. We can determine a product's efficacy by evaluating whether it can protect against certain drops in temperature. In addition, we can determine if the environmental constraints of a product are acceptable for its intended environmental conditions for usage. For example, our heat transfer simulation indicates that the nose can reach temperatures as low as 4F. We can test the efficacy of frostbite prevention products such as Dermatone and Akilhiver, skin protection creams, by evaluating if these products can protect against such a large temperature decrease. In addition, products such as cold resistant fabrics for use in ski masks, or Balaclavas, for extremely cold temperatures can also be evaluated for efficacy and environmental constraints utilizing data from the fluid flow simulation. According to the fluid flow simulation, the nose experiences the brunt of the free stream velocity due to its prominent topography. Thus, a ski mask designed for cold prevention must use materials that provide the highest amount of protection in the nasal region. Appendix C includes a more in-depth analysis of products utilized for frostbite protection based on the data obtained from our study.

Through fluid flow and heat transfer simulations performed within COMSOL, we identified the facial regions most susceptible to frostbite. These regions included the cheeks, nose, and chin. Simulations allowed us to study the effects of frostbite at several different layers of abstraction, allowing us to better understand the phenomena of frostbite. Simulations also enabled us to determine that the nose is the most susceptible facial region to developing frostbite. By providing scientific evidence for the particular facial regions that should be protected from exposure in extremely cold temperatures and high winds, we can reduce the occurrence of frostbite worldwide.

Appendix A: Parameters

Table 4. Apparent Heat Capacity

Temperature (K)	C_{pa} (J/K)
18	4180
248	4180
261	5000
265	10000
265	20000
269	80000
270	44000
270.5	20000
271	4180
333	4180

Table 4. Thermal Conductivity

Temperature (K)	k (W/(m*K))
18	0.627
223	0.627
248	0.62
255	0.6
260	0.55
270	0.27
272	0.22
273	0.209
333	0.209

Note: Apparent heat capacity and thermal conductivity are provided from Assignment 1; Finger tissue.

Appendix B: Mesh Convergence

In order to reduce discretization error and build confidence in the solution obtained, a mesh convergence was performed manually. Discretization error occurs in COMSOL due to the software's inability to perform computations at every point in the domain. Instead, COMSOL must utilize a mesh made up of discrete points and perform computations at these points. Generally, as the mesh utilized in the computational domain increases its number of elements, the discretization error is reduced. Mesh with a large number of elements is defined as a fine mesh, while a mesh with a large number of elements is defined as a coarse mesh. A mesh convergence is performed by evaluating the minimum number of mesh elements that can be utilized so as not to affect the results of the simulation.

In our model, two free tetrahedrals were created to control the mesh size. They were both calibrated for general physics using predefined options.

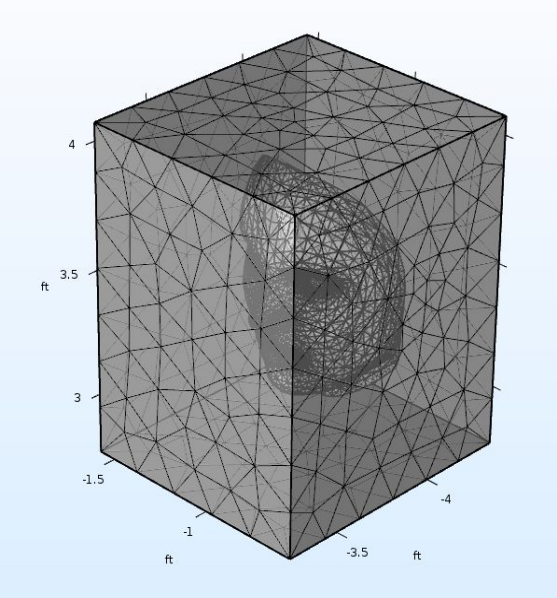

Figure 17 Example of mesh. Domain 2 is set to be normal, domain 1 is set to be coarse.

To evaluate the mesh convergence, we used the initial conditions of wind velocity 6.705m/s and temperature 241.48K. The simulation was run for 6 different mesh densities for an exposure time of 300s. For consistency, we meshed both the face and air domain with the same mesh density. Below is a plot of the nose temperature at 300s versus mesh elements. As shown, the temperature does not vary too much for meshes that have similar number of elements. However, the Finer mesh, which has more than double the number of elements than Fine mesh, outputs a temperature that is lower than all the other meshes. The difference between the temperatures outputted by the Finer and Fine mesh is -0.15, which has a percent difference of 0.057% (Figure 18).

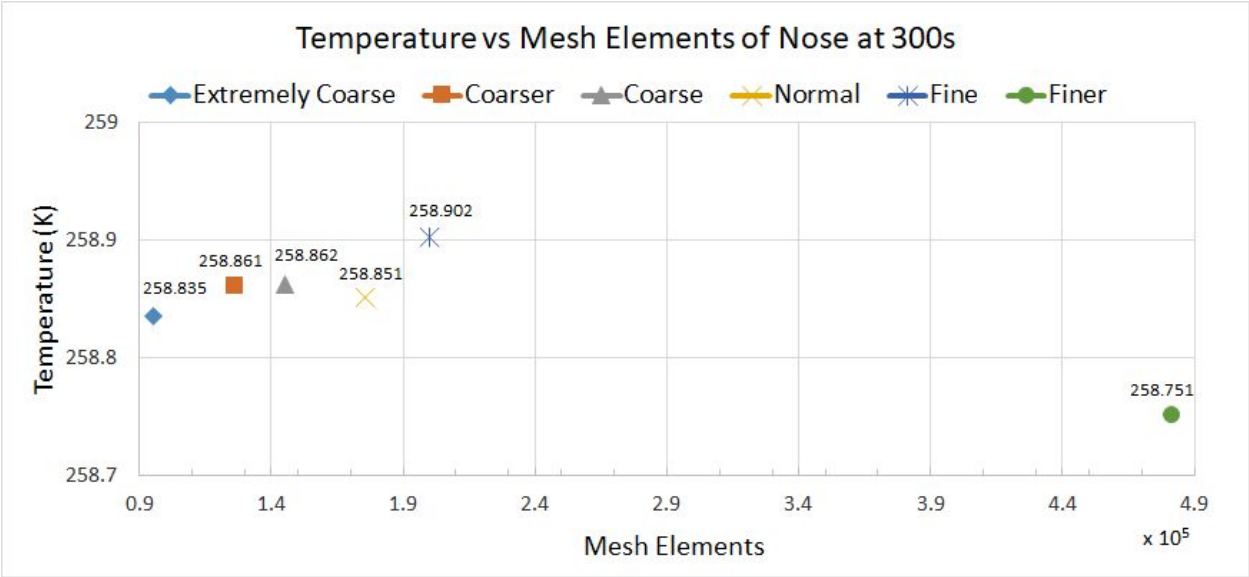

Figure 18 Mesh convergence plot. Temperature of the Nose at 300s varies as the elements increase.

In addition, we conducted mesh convergence by showing different temperature profiles with different mesh densities.

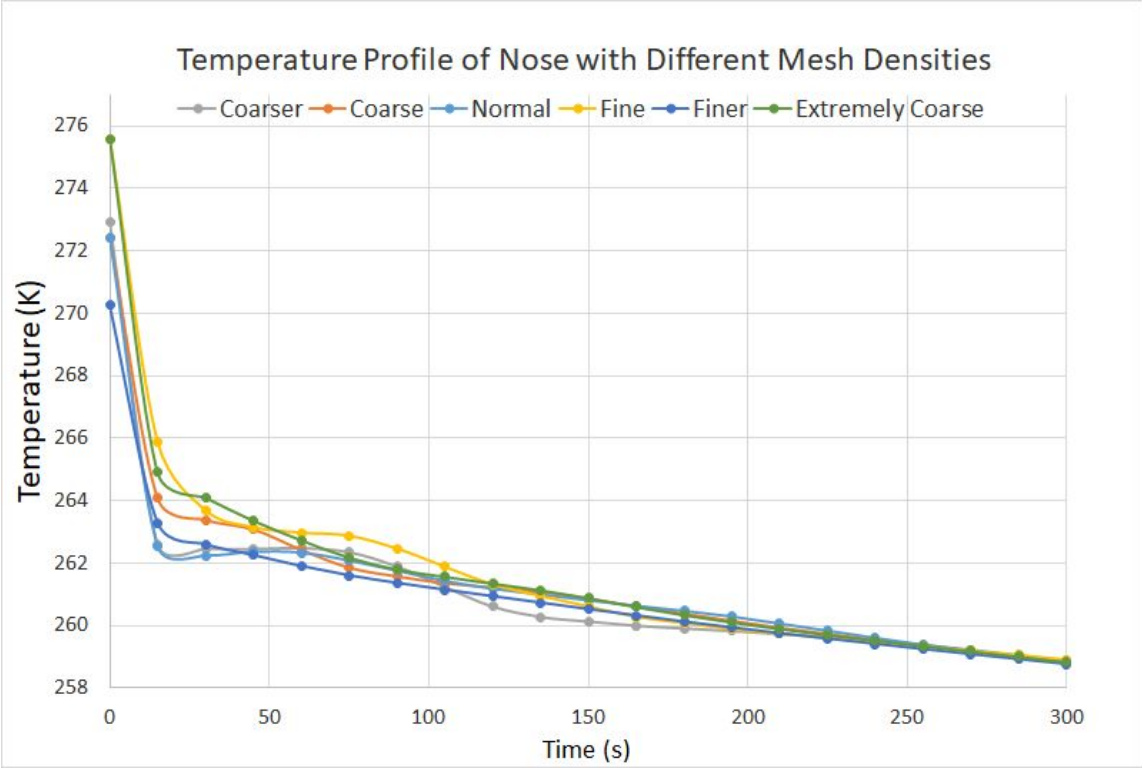

Figure 19. Temperature Profile of Nose With Different Mesh Densities.

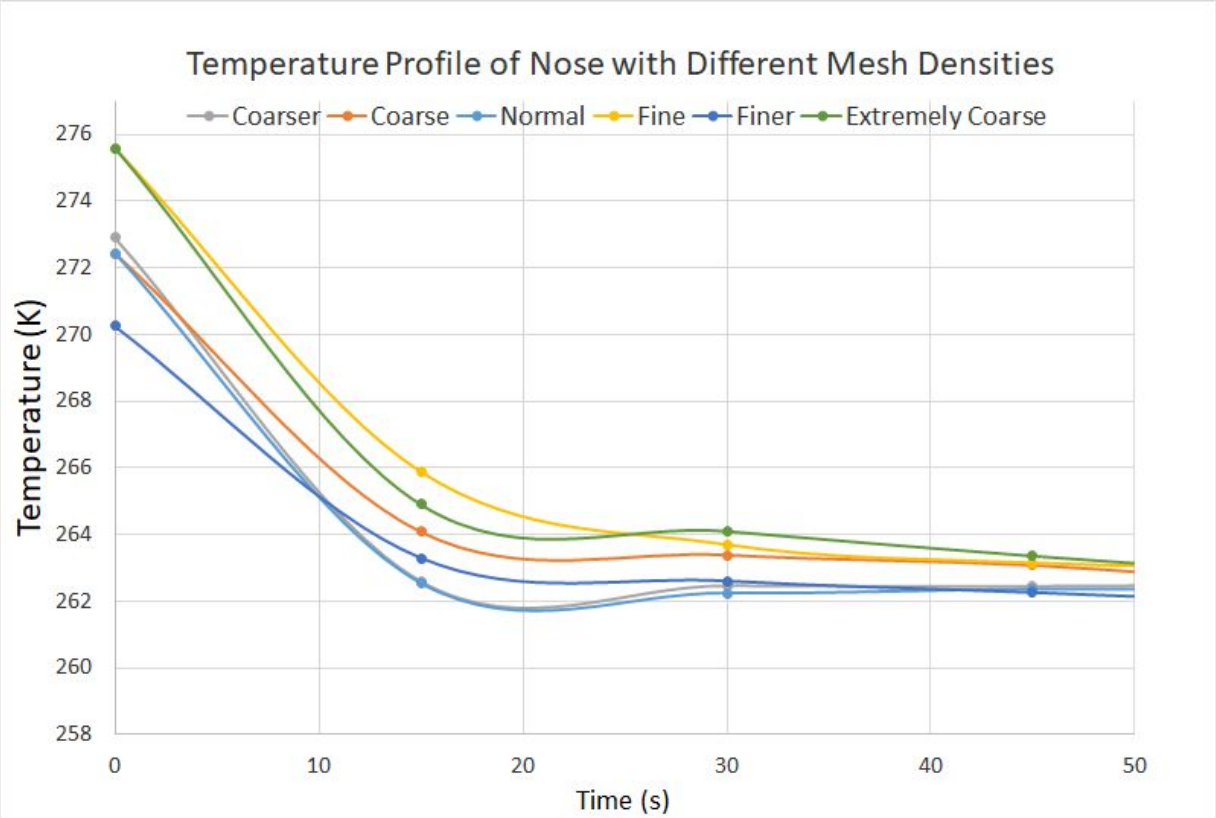

Figure 20. Temperature profile of -25F and 15mph for the first 50 seconds. Fine mesh is shown as the smoothest.

We concluded that since all mesh densities converge at 50s and there is slight difference in the beginning. Using the mesh convergence plot of temperature vs mesh elements and temperature vs time at different mesh densities, we concluded that fine element would give us the smoothest results.

Appendix C: Product Analysis

Facial modeling demonstrates the most critical area to be protected against frostbite is the nose. Any cold weather face protection should, whether it be a cream like Dermatone, or a full face mask should first protect the nose. Listed below is analysis for different methods for frostbite protections in relation to the temperature profiles found in Figures four, five, and six.

Dermatone: Dermatone and other similar products are a form of high viscosity gels that coat the skin and provide frostbite protection. Gels are favored by sportsmen such as skiers and hunters who desire protection from the cold but do not want to limit visibility. Gels have the advantage of being low cost but also have several disadvantages. Gels only work in the areas of skin where there has been a direct application of the gel. Dermatone will provide protection down to -4 F but Figure 4 shows that with a 10 mph wind, which produces a wind chill temperature of -22 F, the temperature of the skin drops rapidly after as little as 50 seconds of exposure. This would likely produce frostbite in as little as 30 minutes of exposure. Dermatone should only be used in more moderately cold temperatures and for activities where exposure times are limited (Lehmuskallio, 2001).

Balaclava: Without a doubt, the Balaclava, or ski mask provides the best protection for the nose and the entire face since all skin is covered by the Balaclava material, except for the skin around the lips and eyes which have warming due to ample blood flow. Balaclavas are ideal for long duration exposure in extremely cold temperatures but with balaclavas available in many different fabrics and price ranges, consideration should be taken on what type of exposure to extreme cold temperatures the wearer expects to endure ("The 8 Best Balaclavas of 2019." 2019).

> **Wool, Acrylic, and Merino Wool:** These types of Balaclavas are readily available and relatively inexpensive. The tight weave of the fabric serves as a barrier, and products like Merino wool offer some moisture wicking and breathability of the fabric. Merino wool, sometimes called WoolX is considered superior to wool and acrylic providing protection down to -30F. With a 10 mph wind, a -30F wind chill could be experienced at near 0F temperatures. The Army Research Lab in Natick, MA recently discovered the moisture wicking properties of Merino wool have been overstated and suggests not using Merino wool in high moisture environments even in temperatures as high as +39F since the fabric can trap moisture and keep it near the skin, increasing susceptibility to cold weather injuries. The wind chill chart in Figure 10 shows that a 10-knot wind will produce wind chill in the +25F range in temperatures as high as +35F, with a rapid skin temperature drop occurring in as little as 50 seconds of exposure time. This corresponds with the finding from our modeling which shows frostbite is likely to occur at +25F with prolonged exposure times. Modeling shows wool and synthetic wool products should only be used for a short duration in temperatures relatively near freezing, and only in dry air.
>
> **Polartec:** Polartec fabrics, often called fleece, are made from thin synthetic fibers weaved together then napped. A Balaclava made from Polartec provides cold weather protection down to -40F, while still offering breathability and moisture wicking and

according to the manufacturer can be comfortably worn in temperatures as high as +40F. The Army uses Polartec fabrics as the basis for their Extreme Cold Weather Clothing System (ECWCS) for soldiers expected to experience extremely cold weather temperatures for long durations. Polartec's effectiveness in a large temperature range it versatile and likely ideal for most extreme cold weather applications. According to Figure 4, the wearer of a Polartec Balaclava would see no reduction in skin temperature despite continual exposure to temperatures as low as +4F. The increased popularity of these products has lowered their price and according to Amazon, a genuine Polartec Balaclava can be purchased for as little as $45.00 (Defense Technical Information Center, 1986).

Nanowires: Although Polartec is an excellent system, the entire ECWCS still weighs 18 lbs and becomes uncomfortable with continual wear. The latest cold weather technology fabrics that will likely find its way into commercial applications are called Nanowires. Nanowires are silver wires embedded in the fabric that reflect heat back to the wearer. The wires are energized by a small three-volt battery that is just about the size of a watch battery. The wires are so effective, that the fabric can be heated to temperatures as high as +230F. The fabric is also impregnated with a moisture-wicking hydrogel. A Nanowire embedded Balaclava could likely provide frostbite protection in the coldest temperatures recorded on earth, but this technology is still in the experimental phase and prohibitively expensive at the current time. Perhaps someday Nanowires will make the risk of facial frostbite a thing of the past ("Army Develops Cloth That Could Drastically Improve Cold-Weather Uniforms," 2017).

.

References

1. https://journals.ametsoc.org/doi/full/10.1175/BAMS-D-16-0259.1
2. https://www.thedailybeast.com/it-takes-just-60-seconds-to-get-frostbite-in-chicagos-polar-vortex
3. https://www.engineeringtoolbox.com/convective-heat-transfer-d_430.html
4. https://www.cheric.org/files/education/cyberlecture/e201501/e201501-201.pdf
5. https://docs.google.com/document/d/13R-kFQ2SJuFx1pKjZ8wmcAu8lttPM7vSA1MyK-vAFPc/edit
6. https://www.sciencedirect.com/science/article/pii/S2300396017300113
7. https://app.knovel.com/web/view/khtml/show.v/rcid:kpIMTPABS6/cid:kt007UDH31/viewerType:khtml//root_slug:bsection-i-essential-stepsb/url_slug:section-i-essential-steps?b-toc-cid=kpIMTPABS6&b-toc-root-slug=&b-toc-url-slug=section-i-essential-steps&b-toc-title=Introduction%20to%20Modeling%20of%20Transport%20Processes%20-%20Applications%20to%20Biomedical%20Systems&page=36&view=collapsed&zoom=1
8. https://www.sciencedirect.com/topics/medicine-and-dentistry/skin-blood-flow
9. https://www.physlink.com/education/askexperts/ae420.cfm
10. https://www.comsol.com/blogs/how-to-reuse-a-deformed-shape-as-a-geometry-input/
11. https://www.mayoclinic.org/diseases-conditions/frostbite/symptoms-causes/syc-20372656
12. https://www.weather.gov/safety/cold-wind-chill-chart
13. https://archive.org/details/DTIC_ADA190226/page/n9
14. https://taskandpurpose.com/army-develops-cloth-drastically-improve-cold-weather-uniforms
15. http://jultika.oulu.fi/files/isbn9514259882.pdf
16. https://www.tripsavvy.com/best-balaclavas-4156578